Memorias del 2022 Congreso Nacional de Control Automático
12-14 de Octubre, 2022. Tuxtla Gutiérrez, México.

Continuous Model Predictive Control for the Direct Torque Control of a PM Synchronous Motor ⋆

F. González Sáenz * **O. Sandre Hernández** **
J. P. Ordaz Oliver *

* *CITIS, AACyE, ICBI, Autonomous University of Hidalgo State, Pachuca 42184, Hidalgo, Mexico; fbsaenz095@gmail.com, jesus_ordaz@uaeh.edu.mx*
** *CONACYT-UAEH, CITIS, AACyE, ICBI, Autonomous University of Hidalgo State, Pachuca 42184, Hidalgo, Mexico; omar_sandre@uaeh.edu.mx*

Abstract: This paper presents the application of the continuous model predictive control (C-MPC) for the direct torque control (DTC) of a permanent magnet synchronous motor (PMSM). The C-MPC is designed for the direct regulation of the components of the stator flux and the electromagnetic torque of the PMSM. A linear state-space model based on a feedback linearization of the PMSM is used to formulate the controller. The control signals are applied to the PMSM via a power inverter through a pulse width modulator (PWM). The proposed controller is formulated as a constrained optimization problem, where the voltage applied to the motor is selected as the control input and restricted to the linear region of the power inverter. Simulation results are presented to demonstrate the effectiveness of the proposed control scheme.

Keywords: Direct Torque Control, Flux Control, PMSM, Model Predictive Control

1. INTRODUCTION

In the field of power electronics, the application of model predictive control (MPC) has been widely accepted in the industry and the academic community. The main advantage of MPC over other control strategies is the natural inclusion of constraints and non linearities in the control design. Moreover, the formulation of a multivariable control is a straightforward task in MPC (Borrelli et al. (2017)).

MPC is based on the formulation of an optimal control problem which is solved in real-time. The problem formulation strongly depends on the mathematical model of the plant, which is the main disadvantage of MPC due to parameter variations and unmodeled dynamics. On the other hand, the application of MPC was initially performed for relatively slow systems. However, with the advent of more powerful digital platforms, MPC has been successfully applied to systems with faster dynamics, such as electrical drives (Karamanakos et al. (2020)).

In the field of electrical drives, MPC has evolved into two well established categories: the continues MPC (C-MPC) (Wallscheid and Ngoumtsa (2020); Hammoud et al. (2022); Kim et al. (2014); Lascu et al. (2012)); and the finite set MPC (FS-MPC) (Nguyen and Jung (2018); Sandre-Hernandez et al. (2018); Xie et al. (2015)). In both control schemes, the main objective is to minimize a predefined cost function to select the optimal control, referred to as the optimal voltage vector in the following, for application in the AC motor. The main difference between C-MPC and FS-MPC is the voltage vector to be optimized, while in C-MPC the optimal control results in a continuous voltage vector applied by a pulse width modulator (PWM); in the FS-MPC the direct control of the switching states of the power converter is performed for the optimization of the voltage vector applied to the machine.

The application of C-MPC to different AC machines has been reported in the literature (Wallscheid and Ngoumtsa (2020); Hammoud et al. (2022); Kim et al. (2014); Lascu et al. (2012); Li et al. (2021); Choi et al. (2016); Kim et al. (2013)). In particular, the permanent magnet synchronous motor (PMSM) is studied in this paper. The PMSM is a popular machine due to its high efficiency, high power density, high dynamic response, and compact size (Krishnan (2017)). These characteristics make the PMSM ideal for high dynamic applications. However, for

⋆ This article is financed through the annual operational project 2022 (PAO 2022) with code 0503 of the Autonomous University of Hidalgo State.

a proper operation, the PMSM is commonly controlled by the classical field-oriented control (FOC) or direct torque control (DTC) (Finch and Giaouris (2008)).

An alternative to FOC and DTC is the application of C-MPC for the PMSM. Typically, the C-MPC is formulated for the regulation of stator current components in the rotor frame $d-q$ (Wallscheid and Ngoumtsa (2020); Hammoud et al. (2022); Kim et al. (2014)). This approach is similar to FOC, where the d current component is calculated according to the operation of the controller, for example, maximum torque per ampere, or flux weakening operation; and where the q component is used to control indirectly the torque developed by the PMSM.

In some applications it is desirable to control the torque and stator flux of the PMSM directly, for example, direct traction drives. Conventionally, torque and stator flux control relays on the FS-MPC, however, the C-MPC can be formulated for the control of torque and flux of the PMSM. Recently, nonlinear control techniques based on feedback linearization have been applied to the torque and flux control of the PMSM. In Li et al. (2021) a feedback linearization DTC is presented for the control of an interior PMSM, this controller improves the torque and flux response based on sliding mode control. In Choi et al. (2016) a feedback linearization DTC is presented for the control of an interior PMSM, in this work a state error vector is used to design the controller, which decays asymptotically to zero. In Lascu et al. (2012) a feedback linearization DTC with a variable structure control is presented, this controller is used to improve the robustness of the control against errors and modeling uncertainties.

In this paper, feedback linearization is used for the formulation and application of the C-MPC in the DTC of a PMSM. In contrast with previous feedback linearization works, the application of the C-MPC allows to include constraints on the voltage applied to the PMSM. An equivalent linear model of the PMSM is obtained by the feedback linearization presented in Lascu et al. (2012). This model is then used to develop a constrained C-MPC for the regulation of the torque and flux of the PMSM. Simulation results of the proposed control schemes in Matlab/Simulink are presented to demonstrate the effectiveness of the proposed control scheme.

2. MATHEMATICAL MODEL OF THE PM SYNCHRONOUS MOTOR

2.1 Continuous-time model of the PMSM

The machine under study is a surface PMSM, which can be modeled in the rotor reference frame $d-q$. Thus, the voltage equations of the PMSM can be described as in Krishnan (2017):

$$\begin{aligned} u_{sd} &= R_s i_{sd} + L_{sd}\tfrac{d}{dt} i_{sd} - p\omega_m \cdot L_{sq} i_{sq}, , \\ u_{sq} &= R_s i_{sq} + L_{sq}\tfrac{d}{dt} i_{sq} + p\omega_m \left(L_{sd} i_{sd} + \psi_{PM}\right), \end{aligned} \tag{1}$$

where L_{sd} and L_{sq} are the inductance in the $d-q$ axis respectively; i_{sd} and i_{sq} are $d-q$ axis currents; ψ_{PM} is the permanent magnet flux of the rotor; R_s is the stator resistance for both $q-d$ axis; ω_m is the mechanical speed; and u_{sd}, u_{sq} are the $d-q$ axis voltages. Since the PMSM under study is a surface PMSM, it is considered that $L_s = L_{sd} = L_{sq}$. Then, the following equation describes the electromagnetic torque M_e:

$$M_e = \tfrac{3}{2} p \psi_{PM} i_{sq}, \tag{2}$$

where p is the pair of poles. Finally, the equations that describes the electromagnetic flux are given by:

$$\begin{aligned} \psi_{sd} &= L_s i_{sd} + \psi_{PM}, \\ \psi_{sq} &= L_s i_{sq}, \\ \psi_s &= \sqrt{\psi_{sd}^2 + \psi_{sq}^2}, \end{aligned} \tag{3}$$

where ψ_{sd} and ψ_{sq} are the components of the stator flux in the $d-q$ axis respectively; and ψ_s is the magnitude of the stator flux.

The mathematical model described by (1)-(3) is used to obtain the dynamic behavior of the torque and flux of the PMSM. The derivative of (2) and (3), in combination with (1), can be written as in Lascu et al. (2012):

$$\begin{aligned} \tfrac{d}{dt} M_e &= K_T u_{sq} - \tfrac{R_s}{L_s} M_e - K_T p \omega_m \psi_{sd}, \\ \tfrac{d}{dt} \psi_s &= 2\psi_{sd} u_{sd} + 2\psi_{sq} u_{sq} + 2\tfrac{R_s}{L_s} \psi_{PM} \psi_{sd} - 2\tfrac{R_s}{L_s} \psi_s, \end{aligned} \tag{4}$$

where $K_T = \frac{3}{2} p \psi_{PM} / L_s$. The model described by (4) presents coupled dynamics. A linear model of the PMSM can be obtained by feedback linearization. By defining the new variables:

$$\begin{aligned} w_q &= K_T u_{sq} - K_T p \omega_m \psi_{sd}, \\ w_d &= 2\tfrac{R_s}{L_s} \psi_{PM} \psi_{sd} + 2\psi_{sd} u_{sd} + 2\psi_{sq} u_{sq}, \end{aligned} \tag{5}$$

the state-space model for the torque and flux control of the PMSM can be written as:

$$\tfrac{d}{dt} \mathbf{x}(t) = \mathbf{A_i} \mathbf{x}(t) + \mathbf{B_i} \mathbf{u}(t), \tag{6}$$

where

$$\mathbf{A_i} = \begin{bmatrix} -\frac{R_s}{L_s} & 0 \\ 0 & -2\frac{R_s}{L_s} \end{bmatrix}, \quad \mathbf{B_i} = \begin{bmatrix} 1 & 0 \\ 0 & 1 \end{bmatrix}, \tag{7}$$

$$\mathbf{x(t)} = \begin{bmatrix} M_e \\ \psi_s \end{bmatrix}, \quad \mathbf{u}(t) = \begin{bmatrix} w_q \\ w_d \end{bmatrix}. \tag{8}$$

2.2 Discrete-time model of the PMSM

C-MPC is performed in the discrete-time domain, therefore, the continuous state-space model of the PMSM given by (6) is converted to its equivalent discrete-time model. The sampling period can be considered small enough to discretize by the application of the Euler forward method. Additionally, an embedded integrator is used in the model to reduce the steady-state error. Then, by taking the discrete difference of the state $\Delta \mathbf{x}_m(k)$ and the control $\Delta \mathbf{u}(k)$ as:

$$\begin{aligned} \Delta \mathbf{x}_m(k) &= \mathbf{x}_m(k) - \mathbf{x}_m(k-1), \\ \Delta \mathbf{u}(k) &= \mathbf{u}(k) - \mathbf{u}(k-1), \end{aligned} \tag{9}$$

the discrete state-space model of the PMSM is formulated as in Wang (2009):

$$\begin{bmatrix} \Delta\mathbf{x}_m(k+1) \\ \mathbf{y}(k+1) \end{bmatrix} = \begin{bmatrix} \mathbf{A}_m & \mathbf{o}_m^T \\ \mathbf{C}_m\mathbf{A}_m & \mathbf{I}_{q\times q} \end{bmatrix} \begin{bmatrix} \Delta\mathbf{x}_m(k) \\ \mathbf{y}(k) \end{bmatrix} + \begin{bmatrix} \mathbf{B}_m \\ \mathbf{C}_m\mathbf{B}_m \end{bmatrix} \Delta\mathbf{u}(k), \tag{10}$$

$$\mathbf{y}(k) = \begin{bmatrix} \mathbf{o}_m & \mathbf{I}_{q\times q} \end{bmatrix} \begin{bmatrix} \Delta\mathbf{x}_m(k) \\ \mathbf{y}(k) \end{bmatrix},$$

where $\mathbf{A}_m = \mathbf{I} + \mathbf{A}_i T_s$; $\mathbf{B}_m = \mathbf{B}_i T_s$; T_s is the sampling time; q is the number of outputs; and o_m is a zero matrix of appropriate dimensions. Equation (10) can be rewritten in a compact form as:

$$\begin{aligned} \mathbf{x}(k+1) &= \mathbf{A}\mathbf{x}(k) + \mathbf{B}\Delta\mathbf{u}(k), \\ \mathbf{y}(k) &= \mathbf{C}\mathbf{x}(k). \end{aligned} \tag{11}$$

3. DIRECT TORQUE CONTROL OF THE PMSM BASED ON C-MPC

The stator flux and the torque of the PMSM can be controlled directly by the application of C-MPC, however, a cascade control is commonly used in the speed and position control. In the proposed control scheme, two control loops are used. An outer loop is used for the speed regulation of the PMSM, an inner loop based on the C-MPC is used for the regulation of the stator flux and the torque of the PMSM. The control actions obtained from the C-MPC are converted by using (5) to the voltage components u_{sd} and u_{sq} and are applied to the PMSM using the space vector pulse width modulation (SV-PWM). A simplified diagram block of the proposed control scheme is shown in Fig. 1.

3.1 Speed loop control

The outer loop is used for the regulation of the mechanical speed. The mechanical model can be described as:

$$\tfrac{d}{dt}\omega_m = \tfrac{1}{J}\left(M_e - M_L\right), \tag{12}$$

where J is the rotor inertia; and M_L is the load torque. The control design has been presented in Moreno Beltran et al. (2020), and in this work, the discrete approximation of the speed controller is used. The control action for the speed regulation is given by:

$$\begin{aligned} e_\omega &= \omega_{mref} - \omega_m + k_\omega \int \left(\omega_{mref} - \omega_m\right) dt, \\ M_{eref} &= J\left(k_1 e_\omega + \tfrac{d}{dt}\omega_{mref} + \tfrac{M_L}{J} + k_\omega\left(\omega_{mref} - \omega_m\right)\right), \end{aligned} \tag{13}$$

where e_ω is the speed regulation error; ω_{mref} and M_{eref} are the reference speed and the reference torque respectively; and k_1, k_ω are positive definite gains. A simple approximation can be obtained by the application of the Euler method, hence, by defining the new variable $e'_\omega = k_\omega \int \left(\omega_{mref} - \omega_m\right) dt$, the discrete control action for the speed regulation is given by:

$$\begin{aligned} e'_\omega(k) &= e'_\omega(k-1) + T_s k_\omega\left(\omega_{mref}(k-1) - \omega_m(k-1)\right), \\ e_\omega(k) &= \omega_{mref}(k) - \omega_m(k) + e'_\omega(k), \\ M_{eref}(k) &= J\big(k_1 e_\omega(k) + \tfrac{M_L(k)}{J} \\ &\qquad + k_\omega\left(\omega_{mref}(k) - \omega_m(k)\right)\big). \end{aligned} \tag{14}$$

It can be seen that (14) relies on the value of M_L, which is commonly unknown. In this paper, the load torque is known in advance. However, to avoid the implementation of torque sensors, M_L can be estimated by a state-observer as in Zhu et al. (2000).

3.2 Torque and Flux Control based on the C-MPC

The C-MPC strategy is used to achieve the torque and flux control objective:

$$\lim_{k\to\infty} M_e(k) = M_{eref}, \ \lim_{k\to\infty} \psi_s(k) = \psi_{sref}, \tag{15}$$

where ψ_{sref} is the stator flux reference. In the C-MPC, the discrete state-space model of the PMSM given by (10) is used to predict the behavior of the state variables at a fixed time window referred to as the prediction horizon N_P; and to predict the behavior of the output variable at a fixed time window referred to as the control horizon N_c. Hence, by using the model described by (10), the prediction of the state and the output can be obtained recursively for any arbitrary value of k respectively as:

$$\begin{aligned} \mathbf{x}(k_i + N_p \mid k_i) &= \mathbf{A}^{N_p}\mathbf{x}(k_i) \\ &\quad + \sum_{i=0}^{N_c-1} \mathbf{A}^{N_p-i-1}\mathbf{B}\Delta\mathbf{u}(k_i+i), \\ \mathbf{y}(k_i + N_p \mid k_i) &= \mathbf{C}\mathbf{A}^{N_p}\mathbf{x}(k_i) \\ &\quad + \sum_{i=0}^{N_c-1} \mathbf{C}\mathbf{A}^{N_p-i-1}\mathbf{B}\Delta\mathbf{u}(k_i+1), \end{aligned} \tag{16}$$

where k_i is the initial sampling time for the prediction of the variables, and the representation $(k_i + N_p|k_i)$ denotes the prediction from the sampling time k_i. Then, the prediction of the state variables is used to minimize a predefined cost function to obtain the optimal control action to be applied to the PMSM.

By using the stator flux and the torque as the state variables, the state vector used in the incremental model can be defined as:

$$\mathbf{x}(k) = \Big[M_e(k) - M_e(k-1), \psi_s(k) - \psi_s(k-1), M_e(k), \psi_s(k)\Big]^T \tag{17}$$

The torque and flux reference can be considered constant within the prediction horizon. Then, by defining the reference vector as:

$$\bar{\mathbf{x}}(k) = \Big[0, 0, M_{eref}(k), \psi_{sref}(k)\Big]^T, \tag{18}$$

where $M_{eref}(k) = M_{eref}$, and $\psi_{sref}(k) = \psi_{sref}$. The torque reference is defined by the speed control loop given by (14). On the other hand, the flux reference can be obtained from the torque equation. The torque of the PMSM can be rewritten in terms of the stator flux as:

$$M_e = \frac{3}{2} p \psi_{PM} \left[\frac{1}{L_s} \sqrt{\psi_s^2 - L_s i_{sd}} \right]. \quad (19)$$

The maximum torque of the PMSM can be obtained considering $\partial M_e / \partial i_{sd} = 0$, which results in:

$$\psi_{sref}^2 = \psi_{PM}^2 + L_s \left[\frac{2 * M_{eref}}{3 p \psi_{PM}} \right]. \quad (20)$$

Then, the reference tracking error can be defined as:

$$\mathbf{e}(k) = \mathbf{x}(k) - \bar{\mathbf{x}}(k). \quad (21)$$

The objective of C-MPC is to minimize the reference tracking error given by (21), which is equivalent to bring the predicted output of the system (torque and flux of the PMSM) as close as possible to the reference. In order to bring the error close to zero, the optimal control action $\Delta \mathbf{u}$ which minimize the cost function given by (22) need to be calculated.

$$\begin{aligned} \mathbf{J}(\mathbf{e}, \Delta \mathbf{u}) = & \sum_{j=1}^{N_p} \mathbf{e}\left(k_i + j \mid k_i\right)^T \mathbf{Q} \mathbf{e}\left(k_i + j \mid k_i\right) \\ & + \sum_{j=0}^{N_p} \Delta \mathbf{u}\left(k_i + j\right)^T \mathbf{R} \Delta \mathbf{u}\left(k_i + j\right), \end{aligned} \quad (22)$$

where $\mathbf{Q} \geq 0, \mathbf{R} > 0$ are given are matrices of appropriate dimensions. It is well known that the unconstrained solution for the optimal $\Delta \mathbf{u}$ of $\mathbf{J}$ can be obtained by solving $\partial \mathbf{J} / \partial \Delta \mathbf{u} = 0$. However, in the proposed control scheme, the control action must lie in the lineal region of the SVM-PWM. Thus, a constraint is imposed for the control action, i.e., the $d-q$ voltage components applied to the PMSM. At any discrete-time instant, the following constraint holds for the solution of the optimal problem:

$$\sqrt{u_{sd}^2 + u_{sq}^2} \leq \frac{m_{index}}{\sqrt{3}} U_{DC}, \quad (23)$$

where $m_{index} = 0.907$ is the index modulation for the SV-PWM, and U_{DC} is the voltage of the DC-link of the power inverter. This leads to the constrained optimization problem given by:

$$\begin{aligned} & \min_{\Delta \mathbf{u}} \mathbf{J}(\mathbf{e}, \Delta \mathbf{u}) \\ & s.t. (23) \end{aligned} \quad (24)$$

Dynamic programming is required to solve (24). In this paper, Hildreth's quadratic programming algorithm is used (Iusem and De Pierro (1990)). The optimal solution will lead to the control trajectory given by $\Delta \mathbf{u}$, therefore, the principle of receding horizon control is applied to obtain only the first element of the control trajectory for application in the PMSM. This leads to the final control action given by:

$$\mathbf{u}(k) = \mathbf{u}(k-1) + \begin{bmatrix} 1 & 0 \\ 0 & 1 \end{bmatrix} \Delta \mathbf{u}. \quad (25)$$

Finally, the voltage components u_{sd} and u_{sq} are obtained by using (25) in combination with (5) and are applied to the PMSM via the SV-PWM. For the C-MPC, the tuning parameters are N_p, N_c, $\mathbf{Q}$ and $\mathbf{R}$; and need to be adjusted according to the desired performance. N_p, N_c are selected to cover the transient response of the system, for the PMSM short horizons are commonly employed to reduce the computational burden of the MPC. $\mathbf{Q}$ and $\mathbf{R}$ are selected to balance the trade-off between the tracking error and the control input. For the PMSM control $\mathbf{Q}$ can be chosen as an identity matrix, and $\mathbf{R}$ is selected to balance the effect of the control action in torque and flux of the PMSM.

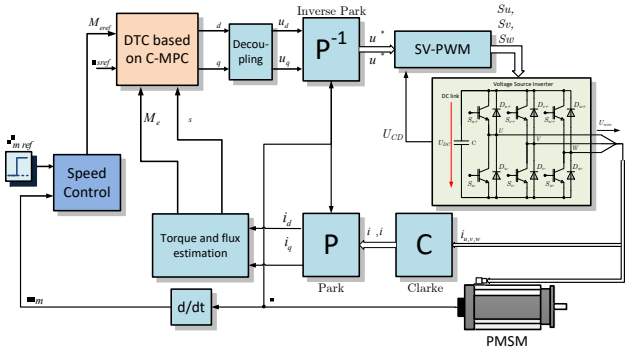

Fig. 1. Simplified diagram of the proposed control scheme

Table 1. Parameters of the PMSM

282V, 3-Φ, PMSM			
Parameter	**value**	**Parameter**	**value**
M_{LN}	4.7 Nm	p	3
R_s	2.41 Ω	Ω_{nom}	3000 Rpm
L_{sd}	24 mH	L_{sq}	24 mH
ψ_{PM}	0.2456 Vs	i_N	3.4 A
J	$3.041 \cdot 10 \quad 3 \quad kgm^2$		

4. SIMULATION RESULTS

This section demonstrates the effectiveness of the proposed control scheme by the simulation of the control scheme described in Fig. 1 through Matlab/Simulink. As shown in Fig. 1, in the control scheme the speed loop is used to determine the torque reference; while the flux reference is given by (20). After the evaluation of the speed control, the measured currents are used to estimate the torque and flux of the PMSM, which are used for the torque and flux control of the PMSM based on the C-MPC. The C-MPC will lead to the linearized variables w_d and w_q, which are used to determine the reference voltage components u_{sd} and u_{sq}. Finally, the reference voltage is synthesized by the SV-PWM for application in the PMSM. The parameters used in the simulation evaluation are adjusted through several simulations, the final values are given as follow: $N_p = 6$, $N_c = 3$, $\mathbf{Q} = \mathbf{C}\mathbf{C}^T$, $\mathbf{R} = [0.05\ 0;\ 0\ 0.001]^T$, $U_{DC} = 450$, $T_s = 100\mu s$; and u_{min}, u_{max} are calculated based on (23).

A comparison with the conventional FS-MPC is presented to verify the performance of the proposed control scheme. FS-MPC is selected as this control scheme uses the same state variables (torque and flux) to control the PMSM, which is not the case of FOC where the currents are controlled. In the FS-MPC, the sampling time used is $T_s = 60\mu s$. The parameters of the PMSM under test are listed in Table 1.

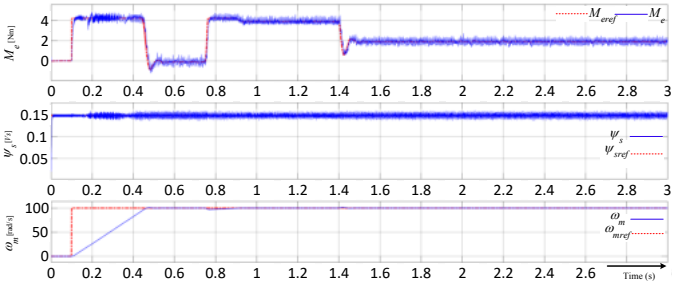

Fig. 2. Results under steady state of the C-MPC control scheme. From top: torque, flux, speed.

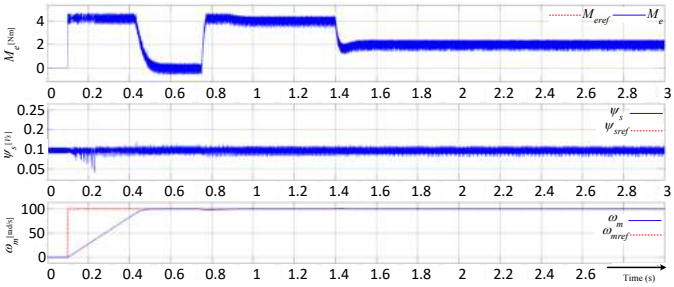

Fig. 3. Results under steady state of the FS-MPC control scheme. From top: torque, flux, speed.

The evaluation under steady-state for the C-MPC and the FS-MPC are shown in Fig. 2 and Fig. 3 respectively. For both evaluations, the speed reference is stepped from 0 to 100 rad/s; and the reference flux is considered constant for all time. A variable load torque is applied to the PMSM, in 0.75s a load torque of $4Nm$ is applied; and at a time of 1.4s, a load torque of $2Nm$ is applied. The simulation results show that both control schemes are robust against the load torque perturbation, and both schemes follow the reference speed accurately. It can be seen that the FS-MPC presents a similar ripple in the controlled variables compared to the C-MPC. In the torque response, the FS-MPC presents a faster dynamic response compared to the C-MPC.

The evaluation under transient-state for the C-MPC and the FS-MPC are shown in Fig. 4 and Fig. 5 respectively. For both evaluations, the speed reference is stepped from 0 to 100 rad/s at a time of 0.1s, then at a time of 1.6s a reference speed of -100 rad/s is applied; for the reference flux is considered constant for all time. Variable load torque is applied to the PMSM: in 0.75s a load torque of $4Nm$ is applied, and at a time of 1.4s a load torque of $2Nm$ is applied. Both control schemes are robust against the load torque perturbation and successfully follow the reference speed. Similar results to the steady-state evaluation are obtained. For the FS-MPC a faster dynamic response is observed compared to the C-MPC. However, the torque and flux ripple is smaller in the FS-MPC in comparison with C-MPC.

Finally, an evaluation of the torque and flux root mean square error (RMSE) is presented in Table 2. The results of the evaluation of the RMSE under steady-state show

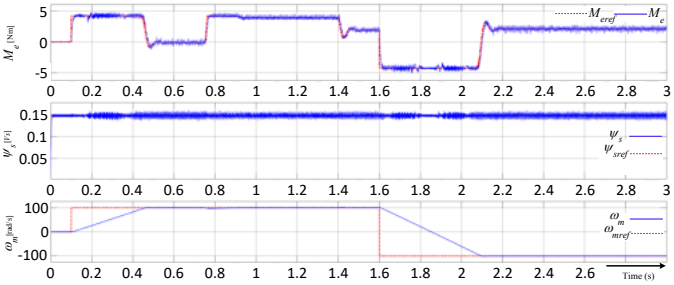

Fig. 4. Results under transient state of the C-MPC control scheme. From top: torque, flux, speed.

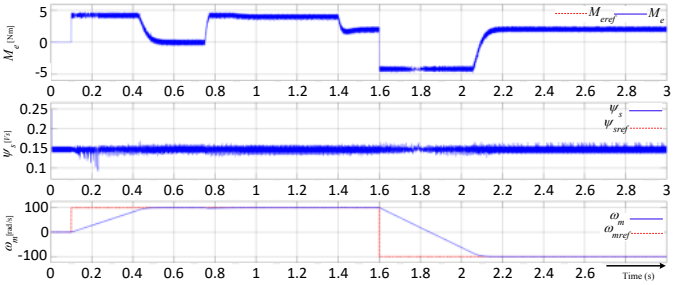

Fig. 5. Results under transient state of the FS-MPC control scheme. From top: torque, flux, speed.

Table 2. Evaluation of the RMSE of the control schemes

Root Mean Square Error			
	Steady state		
	M_e	ψ_s	ω_m
C-MPC	0.2343	0.0060	20.418
FS-MPC	0.2195	0.0065	20.065
	Transient state		
	M_e	ψ_s	ω_m
C-MPC	0.3188	0.0066	51.857
FS-MPC	0.2224	0.0069	50.861

that a similar response in the controlled variables is obtained for the C-MPC and the FS-MPC. Conversely, in transient-state a slightly higher error is obtained for the C-MPC in comparison with the FS-MPC. This is attributed to the slower torque response obtained under the C-MPC. The results in table 2 can be rewritten in percentage ripple. Under steady-state a torque ripple of 4.98% and 4.67%; and a flux ripple of 4.23% and 4.48% for the C-MPC and the FS-MPC is obtained respectively. Under transient-state a torque ripple of 6.78% and 4.73%; and a flux ripple of 4.65% and 4.86% for the C-MPC and the FS-MPC is obtained respectively.

The simulation results have shown that C-MPC and FS-MPC result in a similar performance. However, the sampling time required for the FS-MPC is smaller than the one required for the C-MPC. This can be a disadvantage as a more powerful digital platform is required for the implementation of FS-MPC. In contrast, the C-MPC can be implemented with a larger sampling time, however, a lower sampling time may improve the performance response of the controller. Another advantage of C-MPC is

the application of the reference voltage by using the SV-PWM, which results in a constant switching frequency of the power inverter. Since the FS-MPC control scheme, modifies directly the switching states of the power inverter for the application of the control action, the switching frequency is variable. Moreover, results show that under a larger sampling time, C-MPC results in a similar performance of torque and flux ripple compared to the FS-MPC.

5. CONCLUSION

In this paper, a C-MPC for the direct torque control of a PMSM is presented. Feedback linearization is used to transform the nonlinear model of the PMSM into a linear model for the MPC. Then, a constrained optimal control is formulated for the torque and flux regulation of the PMSM. The performance under the steady and transient state is evaluated through simulation. The results have demonstrated that a similar response is obtained for both control schemes, however, C-MPC requires a higher sampling time for the implementation compared to FS-MPC. Furthermore, C-MPC results in the constant switching frequency of the power inverter, while FS-MPC results in variable switching frequency. Both control schemes are a possible solution for high-performance electrical drives.

ACKNOWLEDGEMENTS

The authors thank to the National Council of Science and Technology (CONACYT), México, for the Master's scholarship given to the first author of this paper.

REFERENCES

Borrelli, F., Bemporad, A., and Morari, M. (2017). *Predictive control for linear and hybrid systems*. Cambridge University Press.

Choi, Y.S., Choi, H.H., and Jung, J.W. (2016). Feedback linearization direct torque control with reduced torque and flux ripples for ipmsm drives. *IEEE Transactions on Power Electronics*, 31(5), 3728–3737. doi: 10.1109/TPEL.2015.2460249.

Finch, J.W. and Giaouris, D. (2008). Controlled ac electrical drives. *IEEE Transactions on Industrial Electronics*, 55(2), 481–491. doi:10.1109/TIE.2007.911209.

Hammoud, I., Hentzelt, S., Xu, K., Oehlschlaegel, T., Abdelrahem, M., Hackl, C.M., and Kennel, R. (2022). On continuous set model predictive control of permanent magnet synchronous machines. *IEEE Transactions on Power Electronics*, 1–1. doi: 10.1109/TPEL.2022.3164968.

Iusem, A.N. and De Pierro, A.R. (1990). On the convergence properties of hildreth's quadratic programming algorithm. *Mathematical programming*, 47(1), 37–51.

Karamanakos, P., Liegmann, E., Geyer, T., and Kennel, R. (2020). Model predictive control of power electronic systems: Methods, results, and challenges. *IEEE Open Journal of Industry Applications*, 1, 95–114. doi: 10.1109/OJIA.2020.3020184.

Kim, S.K., Kim, J.S., and Lee, Y.I. (2013). Model predictive control (mpc) based direct torque control (dtc) of permanent magnet synchronous motors (pmsms). In *2013 IEEE International Symposium on Industrial Electronics*, 1–6. doi:10.1109/ISIE.2013.6563637.

Kim, S.K., Park, H.S., Han, J.H., and Lee, Y.I. (2014). Stabilizing model predictive control for torque control of permanent magnet synchronous motor. In *Proceedings of the 33rd Chinese Control Conference*, 7772–7777. doi:10.1109/ChiCC.2014.6896297.

Krishnan, R. (2017). *Permanent magnet synchronous and brushless DC motor drives*. CRC press.

Lascu, C., Boldea, I., and Blaabjerg, F. (2012). Direct torque control via feedback linearization for permanent magnet synchronous motor drives. In *2012 13th International Conference on Optimization of Electrical and Electronic Equipment (OPTIM)*, 338–343. doi: 10.1109/OPTIM.2012.6231973.

Li, H., Wang, Z., Xu, Z., Wang, X., and Hu, Y. (2021). Feedback linearization based direct torque control for ipmsms. *IEEE Transactions on Power Electronics*, 36(3), 3135–3148. doi:10.1109/TPEL.2020.3012107.

Moreno Beltran, J.P., Sandre Hernandez, O., Morales Caporal, R., Ordaz-Oliver, P., and Cuvas-Castillo, C. (2020). Model predictive torque control of an induction motor with discrete space vector modulation. In *2020 17th International Conference on Electrical Engineering, Computing Science and Automatic Control (CCE)*, 1–6. doi:10.1109/CCE50788.2020.9299193.

Nguyen, H.T. and Jung, J.W. (2018). Finite control set model predictive control to guarantee stability and robustness for surface-mounted pm synchronous motors. *IEEE Transactions on Industrial Electronics*, 65(11), 8510–8519. doi:10.1109/TIE.2018.2814006.

Sandre-Hernandez, O., Rangel-Magdaleno, J., and Morales-Caporal, R. (2018). A comparison on finite-set model predictive torque control schemes for pmsms. *IEEE Transactions on Power Electronics*, 33(10), 8838–8847. doi:10.1109/TPEL.2017.2777973.

Wallscheid, O. and Ngoumtsa, E.F.B. (2020). Investigation of disturbance observers for model predictive current control in electric drives. *IEEE Transactions on Power Electronics*, 35(12), 13563–13572. doi: 10.1109/TPEL.2020.2992784.

Wang, L. (2009). *Model predictive control system design and implementation using MATLAB®*. Springer Science & Business Media.

Xie, W., Wang, X., Wang, F., Xu, W., Kennel, R.M., Gerling, D., and Lorenz, R.D. (2015). Finite-control-set model predictive torque control with a deadbeat solution for pmsm drives. *IEEE Transactions on Industrial Electronics*, 62(9), 5402–5410. doi: 10.1109/TIE.2015.2410767.

Zhu, G., Dessaint, L.A., Akhrif, O., and Kaddouri, A. (2000). Speed tracking control of a permanent-magnet synchronous motor with state and load torque observer. *IEEE Transactions on Industrial Electronics*, 47(2), 346–355. doi:10.1109/41.836350.